

Current changes in tropical precipitation

This article has been downloaded from IOPscience. Please scroll down to see the full text article.

2010 Environ. Res. Lett. 5 025205

(<http://iopscience.iop.org/1748-9326/5/2/025205>)

[The Table of Contents](#) and [more related content](#) is available

Download details:

IP Address: 134.225.158.59

The article was downloaded on 10/04/2010 at 17:03

Please note that [terms and conditions apply](#).

Current changes in tropical precipitation

Richard P Allan¹, Brian J Soden², Viju O John³, William Ingram^{3,4}
and Peter Good³

¹ Department of Meteorology, University of Reading, Earley Gate, PO Box 243, Reading, RG6 6BB, UK

² Division of Meteorology and Physical Oceanography, Rosenstiel School of Marine and Atmospheric Science, University of Miami, 4600 Rickenbacker Causeway, Miami, FL 33149, USA

³ Met Office, FitzRoy Road, Exeter, EX1 3PB, UK

⁴ Department of Physics, University of Oxford, OX1 3PU, UK

E-mail: r.p.allan@reading.ac.uk

Received 1 December 2009

Accepted for publication 23 February 2010

Published 9 April 2010

Online at stacks.iop.org/ERL/5/025205

Abstract

Current changes in tropical precipitation from satellite data and climate models are assessed. Wet and dry regions of the tropics are defined as the highest 30% and lowest 70% of monthly precipitation values. Observed tropical ocean trends in the wet regime (1.8%/decade) and the dry regions (−2.6%/decade) according to the Global Precipitation Climatology Project (GPCP) over the period including Special Sensor Microwave Imager (SSM/I) data (1988–2008), where GPCP is believed to be more reliable, are of smaller magnitude than when including the entire time series (1979–2008) and closer to model simulations than previous comparisons. Analysing changes in extreme precipitation using daily data within the wet regions, an increase in the frequency of the heaviest 6% of events with warming for the SSM/I observations and model ensemble mean is identified. The SSM/I data indicate an increased frequency of the heaviest events with warming, several times larger than the expected Clausius–Clapeyron scaling and at the upper limit of the substantial range in responses in the model simulations.

Keywords: global water cycle, satellite data, climate models, rainfall extremes, trends, climate change

1. Introduction

Substantial changes in the global water cycle are an expected consequence of a warming climate; this is based upon understanding of the governing physical processes and projections made by sophisticated models of the Earth's climate system (Allen and Ingram 2002). Monitoring changes in tropical precipitation is a vital step toward building confidence in regional and large-scale climate predictions and the associated impacts on society (Meehl *et al* 2007).

A number of robust large-scale responses of the hydrological cycle have been identified in models (Held and Soden 2006), relating primarily to increases in low-level moisture with temperature, a consequence of the Clausius–Clapeyron equation. Moisture increases are also thought to lead to the intensification of extreme precipitation (Pall

et al 2007), though sensitivity to model-dependent changes in vertical motion is evident (O’Gorman and Schneider 2009, Gastineau and Soden 2009). Projected rises in global mean precipitation are constrained by radiative–convective balance (e.g. Lambert and Webb 2008) and increase more slowly than atmospheric moisture. Consequences of increased low-level moisture, enhanced horizontal moisture fluxes and the contrasting changes in mean and extreme precipitation include reductions in the strength of the Walker circulation (Vecchi *et al* 2006) and an amplification of global precipitation minus evaporation patterns (Held and Soden 2006), with wet regions becoming wetter at the expense of dry regions (Chou *et al* 2007); many of these anticipated responses have been known about for some time (Mitchell *et al* 1987).

Improving confidence in climate projections demands the use of observations, sampling the many aspects of the

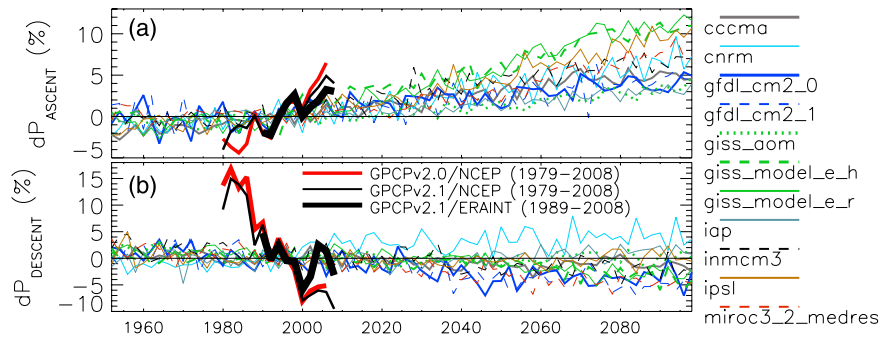


Figure 1. Precipitation anomalies (2 year averages) relative to the mean for the 1989–1999 period over (a) ascending and (b) descending branches of the tropical circulation for CMIP3 coupled atmosphere–ocean models and versions 2.0 and 2.1 GPCP observations applying NCEP or ERA Interim reanalysis vertical motion fields. Updated from Allan and Soden (2007).

global energy and water cycles, to evaluate the relevant processes simulated by models. It is important to establish causes of disagreement, for example relating to observing system deficiencies or inadequate representation of forcing and feedback processes in models. There is observational evidence of increased tropical monthly average moisture and precipitation (Wentz *et al* 2007) and an amplification of extreme precipitation events in response to atmospheric warming (Lenderink and van Meijgaard 2008, Allan and Soden 2008) as well as a contrasting precipitation response over wet and dry regions of the tropics (Zhang *et al* 2007, Allan and Soden 2007, Chou *et al* 2007). While observed precipitation responses appear larger than those simulated by models (Zhang *et al* 2007, Wentz *et al* 2007, Allan and Soden 2008) it is unclear whether this relates to model deficiency, inadequacy in the observing system or is a statistical artefact of the relatively short satellite record (Liepert and Previdi 2009).

The aim of the present work is to identify physically understandable, robust responses of tropical precipitation over the period 1979–2008, using climate models and observations to address the questions: (1) What are current trends in tropical mean precipitation? (2) Are the wet regions becoming wetter at the expense of the dry regions? (3) Are warmer months associated with an increased occurrence of the heaviest precipitation events?

2. Current changes in tropical precipitation

Increases in tropical (30°S–30°N) precipitation since 1979 have been detected using observational data sets (Wentz *et al* 2007, Adler *et al* 2008), in particular for the oceans and over ascending branches of the large-scale circulation (Allan and Soden 2007). The observed responses appear more pronounced than those simulated by coupled atmosphere–ocean climate models with realistic radiative forcings from phase 3 of the Coupled Model Intercomparison Project (CMIP3) and also atmosphere-only experiments (AMIP3) forced with observed sea surface temperature (SST) and sea ice (Wentz *et al* 2007, Allan and Soden 2007) although the results are highly sensitive to the time period and data set used (John *et al* 2009, Liepert and Previdi 2009).

A critical issue with regard to observing current changes in precipitation is the limitations of the satellite data sets. The Global Precipitation Climatology Project (GPCP; Adler *et al* 2008) incorporates a blend of satellite infra-red radiances and predominantly land-based rain gauges since 1979 with microwave ocean measurements from the Special Sensor Microwave Imager (SSM/I) since 1988. In addition to GPCP we also consider the SSM/I-only ocean product (version 6) developed by Wentz *et al* (2007) using the satellite combination: F08 (1987–1991), F11 (1992–1999) and F13 (2000–2008). It is important to note the different sources that contribute to precipitation estimation over land and ocean. In addition, changes in the coverage and calibration issues limit the accuracy in these data sets, in particular for identifying decadal changes. Also critical are the known differences between the satellite data sets and model simulations in representing the frequency distribution of precipitation events (Wilcox and Donner 2007, Field and Shutts 2009) in particular for light rainfall (Sun *et al* 2006, Petty 1997). Acknowledging these limitations, we seek physically understandable, robust responses of the tropical water cycle.

2.1. Ascending and descending regimes

Figure 1 shows precipitation anomalies, relative to the 1989–1999 period, in ascending and descending branches of the tropical circulation, using 500 hPa vertical motion fields from atmospheric reanalyses to sub-sample the observed precipitation and model vertical motion to sample model precipitation. The comparison is identical to Allan and Soden (2007) but also displays an updated version (v2.1) of the GPCP data set (Huffman *et al* 2009) and also uses European Centre for Medium-range Weather Forecast (ECMWF) Interim reanalysis (ERA Interim) data, based upon Uppala *et al* (2005), in place of National Center for Environmental Prediction reanalysis 1 (NCEP; Kalnay *et al* 1996). The update from GPCP version 2.0–2.1 does not alter trends substantially. However, using ERA Interim data reduces the magnitudes of trends, in closer agreement with the models. We propose that the NCEP reanalysis is particularly sensitive to improved representation of vertical motion, with reduced misclassification of GPCP precipitation events in descent regions over time, that may appear to enhance precipitation trends.

Since we cannot quantify to what extent this effect remains when ERA Interim is used, an alternative approach is used.

2.2. Wet and dry regimes

To avoid the use of reanalysis fields, instead percentile bins of precipitation were used to define wet and dry regions. Monthly precipitation values were sorted by intensity, including dry grid-points. Mean precipitation was calculated for the driest 50% of grid boxes and subsequently for each 10% bin ranging from 50 to 60% up to the wettest 10% of grid boxes. Monthly area-weighted means were computed over each bin for the GPCP v2.1 data (1979–2008) and also for ‘run1’ of all AMIP3 models which spanned the entire period 1979–2001: CNRM-CM3, GISS-E-R, INMCM3, IPSL-CM4, MIROC3.2-hires, MIROC3.2-medres, MRI-CGCM2-3.2a, NCAR-CCSM3, HadGEM1 (for details, see www-pcmdi.llnl.gov) and a model ensemble mean. Mean seasonal cycles were subtracted from the resulting time series to reduce the influence of the large changes in solar forcing and associated circulation shifts that are unlikely to be a good surrogate for climate change. Circulation changes are also associated with El Niño although sampling wet or dry regimes will reduce the impact of these changes somewhat. Precipitation trends were calculated using linear least-squares fits. Essentially we seek to quantify the statistical distribution of tropical precipitation and its linear change with time.

Figure 2 shows trends and associated correlation (r) for each percentile bin for the GPCP data, considering the entire period and the 1988–2008 period, when SSM/I ocean data were included. Also shown are trends for the model ensemble mean and range for the nine individual models (grey shading); the ensemble mean correlation coefficient does not lie entirely within the inter-model spread since forming an ensemble can increase correlation as the random unforced component of variability is reduced. Trend magnitudes for GPCP are reduced when excluding the pre-SSM/I period (1979–1987) from the analysis, in closer agreement with the model results. Caution in using pre-1988 GPCP data has been expressed previously (e.g. Adler *et al* 2008) due to issues with inter-calibration of the infra-red satellite radiances and homogeneity associated with changes from infra-red-only to combined infra-red and microwave ocean precipitation retrievals.

Figure 2 shows a clear partition between positive trends above the 60–70th percentile and negative trends below these percentiles for the GPCP and model data. Pall *et al* (2007) found this partition to be sensitive to the latitude chosen, being closer to the 90th percentile for the global mean, although they considered daily model data at approximately 2.7 times CO₂ levels relative to a control. Guided by figure 2, wet and dry regions of the tropics were defined each month as the driest 70% and wettest 30% of grid boxes for each model and satellite data set. Time series were calculated for these regimes over the entire tropics and for land and ocean regions separately.

Figure 3 displays deseasonalized tropical ocean anomalies of SST (HadISST; Rayner *et al* 2003) and precipitation and the wet and dry region precipitation time series for models, GPCP and SSM/I. Linear trends and correlation between precipitation

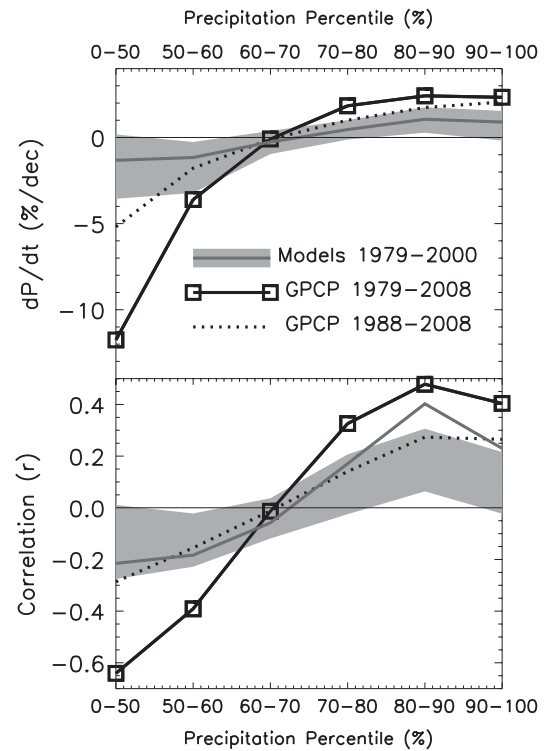


Figure 2. (a) Linear trends in precipitation with time (dP/dt in %/decade) and (b) associated correlation coefficient, r , with percentile bins of tropical monthly precipitation for GPCP data, AMIP3 model ensemble mean and the range for individual models (grey shading).

and SST are presented in table 1; a two-tailed t -test, allowing for autocorrelation (Yang and Tung 1998), was employed to detect significant correlation at the 95% confidence level. Positive precipitation anomalies coincide with warm El Niño years in the models and observations, attributable to the wet tropical region response (figure 3(c)). This relationship is statistically significant with mean precipitation anomalies for GPCP and the model ensemble mean increasing at around 6–10% K⁻¹ depending upon the time period, close to the Clausius–Clapeyron rate, with a spread across the models of 2.9–11% K⁻¹ (table 1). The SSM/I data show a response around twice as large as for GPCP.

Over the tropical oceans, positive precipitation trends are apparent for the wet region (figure 3(c)) and negative trends in the dry regions (figure 3(d)), consistent with Allan and Soden (2007), despite a differing methodology. Observed wet region trends range from 1.8 to 3.0%/decade, overlapping with the upper range of the inter-model spread. The model ensemble trend is also positive, but smaller (1%/decade).

Negative trends in the dry regions for GPCP data are more than halved when excluding the pre-SSM/I period. GPCP anomalies are substantially more positive than model anomalies during 1981–82 and 1984–86, and further analysis is required to assess the accuracy of GPCP data during these periods (Adler *et al* 2008). Nevertheless, GPCP ocean trends for the 1988–2008 period are twice the model ensemble mean trends for the 1979–2001 period despite similar observed SST trends for the two periods (0.06 and 0.08 K/decade respectively). SSM/I data do not show a statistically significant

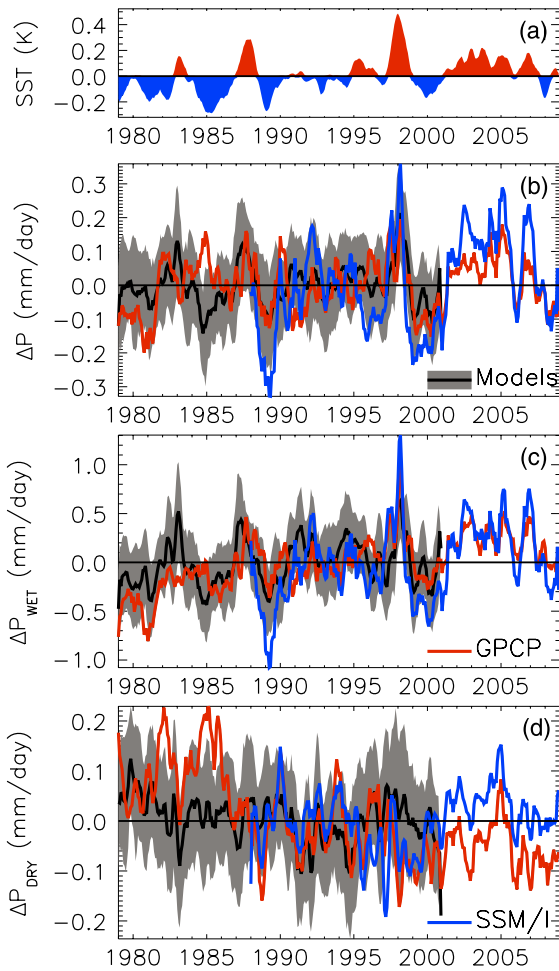


Figure 3. Anomalies of (a) sea surface temperature (SST) and (b) precipitation (P), partitioned into (c) wet and (d) dry regions of the tropical oceans for observations and models (grey shading denotes ± 1 standard deviation).

trend, partly due to positive anomalies since 2000, at odds with the GPCP data. This coincides with the switch between F11 and F13 satellites in the record and may therefore be an inter-calibration issue. Trends over tropical land regions are generally not statistically significant apart from GPCP for the wet regions over the period 1988–2008.

For wet regions over the entire tropics, there is a positive trend of 1.9% per decade for 1988–2008 GPCP data, around double the model ensemble mean trend for 1979–2001. For the NCEP tropical surface temperature trend over 1988–2008 (0.12 K/decade) this corresponds to a sensitivity of 16% K^{-1} for GPCP, above that expected from Clausius–Clapeyron. It is not clear if this super-Clausius Clapeyron response, or others noted elsewhere (Lenderink and van Meijgaard 2008, Liu *et al* 2009), have a physical explanation or whether they are a statistical artefact of the limited observational record (Liepert and Previdi 2009); this is discussed further in section 4.

3. Precipitation extremes in the tropical ocean wet region

We now examine in more detail the wet region precipitation response, using daily data from SSM/I and the models. SSM/I

0.25° × 0.25° data were averaged to a 1° × 1° grid where at least 50% of grid-point data were valid. Ascending and descending satellite over-passes were combined to provide daily estimates. A 2.5° × 2.5° product was generated using bi-linear interpolation, consistent with the climate models which were also interpolated to this common grid.

Allan and Soden (2008) excluded dry grid boxes from analysis of daily rainfall intensity. Since ~70% of the SSM/I grid boxes were found to be dry while in some models all grid boxes contained at least light rainfall, this potentially causes a substantial sampling disparity. Therefore in the present analysis we consider the wettest 20% of all tropical ocean values, including dry grid boxes, in the models and SSM/I data.

The method of Allan and Soden (2008) was applied to calculate monthly percentage anomalies in the frequency of rainfall events in each bin, the percentile boundaries calculated for one year of data from 1990. Each time series is deseasonalized with respect to the mean frequency for each month. This is performed separately for each SSM/I satellite (F08, F11, F13) to avoid satellite inter-calibration issues and to concentrate on interannual anomalies. Results are not substantially altered when considering all satellites as a single record. The calculations are applied to each model (listed in figure 4(f)) separately and averaged to create an ensemble mean (figure 4(c)). Also included is a Clausius–Clapeyron experiment where 12 months of SSM/I daily precipitation data for 1990 were perturbed by 7% K^{-1} anomaly in observed local SST (HadISST).

There is a correspondence between warm El Niño years (figure 4(a)) and a greater frequency of the heaviest rain (above the 94th percentile) in the observations (b) and the model ensemble mean (c). This relationship is partially explained by the simple Clausius–Clapeyron scaling calculated in figure 4(d). However, details of the variation differ between the models and observations: there is a strong anti-correlation ($r = -0.78$) between the frequency of 98–100th percentile and 80–86th percentile rainfall in the models, broadly consistent with Pall *et al* (2007), while the observed relationship is more complex.

In agreement with Allan and Soden (2008), the observed response of intense rainfall frequency to warming is 2–3 times larger than the model ensemble mean sensitivity and the response expected from Clausius Clapeyron (figure 4(e)). The model spread for the most intense rainfall bin is substantial (figure 4(f)), ranging from negative to strongly positive, as noted recently (O’Gorman and Schneider 2009, Gastineau and Soden 2009). Specifically, the CNRM, INMCM, IPSL and MIROC models analysed in the present study appear to capture the observed response of around a 60% increase in the frequency of the wettest 0.2% of events per K warming, while the remaining models do not. Turner and Slingo (2009) found that coupled models (CMIP3) using variants of the Arakawa–Schubert convective parametrization (e.g. CGCM, GFDL, MIROC) tend to produce super-thermodynamic responses of precipitation intensity to warming over India at the time of CO₂ doubling; this is not apparent from the AMIP3 simulations considering the entire tropical oceans in the present study.

Table 1. Linear trends in precipitation (P) and regression with sea surface temperature (SST) for models and observations over tropical land and tropical ocean for wet and dry regimes. * denotes significant correlation at the 95% confidence interval.

Data set	Period	Tropics	Tropical wet	Tropical dry
Interannual relationships: $dP/dSST$ (% K^{-1}), ocean				
GPCP v2.1	1979–2008	$6.4 \pm 1.4^*$	$15.5 \pm 1.7^*$	$-20.3 \pm 3.2^*$
GPCP v2.1	1988–2008	$9.8 \pm 1.8^*$	$13.3 \pm 2.1^*$	-2.3 ± 3.6
SSM/I v6	1988–2008	$21.6 \pm 2.5^*$	$23.1 \pm 2.7^*$	6.1 ± 6.8
Models (range)	1979–2000	$7.7 \pm 0.5^*$ (+2.9 to +11)	$10.1 \pm 1^*$ (+5.6 to +14)	1.8 ± 1.3 (–5.3 to +10)
Trends: dP/dt (%/decade), land + ocean				
GPCP v2.1	1979–2008	0.5 ± 0.2	$2.2 \pm 0.2^*$	$-4.7 \pm 0.4^*$
GPCP v2.1	1988–2008	$1.0 \pm 0.3^*$	$1.9 \pm 0.4^*$	-2.1 ± 0.7
Models (range)	1979–2000	$0.4 \pm 0.1^*$ (–0.4 to +0.7)	$0.9 \pm 0.1^*$ (–0.0 to +1.4)	-0.9 ± 0.3 (–2.2 to +0.1)
Ocean				
GPCP v2.1	1979–2008	0.5 ± 0.3	$2.8 \pm 0.3^*$	$-5.9 \pm 0.5^*$
GPCP v2.1	1988–2008	0.7 ± 0.4	$1.8 \pm 0.5^*$	$-2.6 \pm 0.8^*$
SSM/I v6	1988–2008	$2.8 \pm 0.7^*$	$3.0 \pm 0.7^*$	2.6 ± 1.6
Models (range)	1979–2000	0.3 ± 0.2 (–0.8 to +1.1)	1.0 ± 0.3 (–0.4 to +1.8)	$-1.3 \pm 0.3^*$ (–2.0 to –0.7)
Land				
GPCP v2.1	1979–2008	0.5 ± 0.4	0.7 ± 0.3	-0.6 ± 0.7
GPCP v2.1	1988–2008	1.7 ± 0.6	$2.2 \pm 0.6^*$	-0.6 ± 1.3
Models (range)	1979–2000	0.7 ± 0.4 (–1.0 to +2.1)	0.5 ± 0.3 (–0.9 to +1.6)	1.0 ± 0.7 (–1.9 to +3.8)

Using the SSM/I daily precipitation, it is also interesting to ask, how much of the tropical ocean rainfall variability in figure 3(b) is determined by the heaviest daily rainfall events? Linear fits were calculated between the monthly precipitation anomalies (P), recalculated from the daily data, and perturbed anomalies (P_z) constructed by setting daily precipitation to zero below each percentile threshold, z . The resulting relationship, $P_{94\%} = 0.96P$ ($r = 0.99$), demonstrates the dominance of the heaviest rainfall events measured by SSM/I in determining monthly precipitation variation. Rainfall events above the 99th percentile yield the relationship, $P_{99\%} = 0.66P$ ($r = 0.89$), suggesting that the heaviest 1% of rainfall events contribute roughly two thirds of the tropical ocean precipitation anomalies in the SSM/I data.

4. Conclusions

Tropical precipitation variation is quantified for observations and climate model simulations over the period 1979–2008. The wettest 30% of grid-points and the remaining drier regions are sampled separately. Increased precipitation coincides with warm months associated with El Niño. This is attributable to the wet regions of the tropical ocean with observed precipitation increasing at the rate 13.3–15.5% K^{-1} for GPCP data, at the higher end of the model range (5.6–14.0% K^{-1}) but lower than SSM/I-only data (23.1% K^{-1}). In the SSM/I data, essentially all of the interannual variability in mean tropical ocean precipitation is explained by daily rainfall events above the 94th percentile.

Positive trends in wet regions of the tropical ocean for GPCP are reduced from 2.8%/decade for 1979–2008 to 1.8%/decade for the 1988–2008, where the GPCP record is considered more accurate due to the inclusion of SSM/I data. This is at the upper end of the model range but smaller than SSM/I-only trends. Negative trends in the dry regions of

the tropical ocean are detected for the GPCP data and the models. Again GPCP trend magnitudes are reduced when considering the SSM/I period but are still double the model ensemble mean trend of –1.3%/decade. Discrepancy between observed dry region anomalies since 2000 appears to relate to inhomogeneity of the SSM/I time series. Variation in GPCP precipitation prior to the SSM/I period is also questionable (Adler *et al* 2008) and trends over tropical land are not coherent amongst data sets.

Analysing daily precipitation from SSM/I and model simulations for the wettest 20% of ocean grid boxes demonstrates a clear increase in the frequency of the heaviest rainfall events with warming, consistent with previous analysis (Allan and Soden 2008). The observed frequency of the heaviest 0.2% of rainfall events (including dry grid-points) rises by about 60% K^{-1} of warming. This rise is faster than expected from Clausius–Clapeyron, a result also suggested by Lenderink and van Meijgaard (2008) although their analysis may be sensitive to the transition from large-scale to convective rainfall in hourly data (Haerter and Berg 2009). A super-thermodynamic response is also dependent upon where in the atmospheric profile you are defining the Clausius–Clapeyron scaling (O’Gorman and Schneider 2009). Also, although the effect of large spatial reorganization of circulation systems associated with El Niño are reduced by considering wet regimes, it has yet to be demonstrated that interannual variability is a realistic surrogate for climate change.

Some of the model simulations display a relationship between precipitation extremes and warming that is close to the observations although there is a large spread; previous work has noted the substantial sensitivity of tropical precipitation to changes in vertical motion within such events (Gastineau and Soden 2009, O’Gorman and Schneider 2009, Sugiyama *et al* 2010), likely to relate to differences in model parametrizations (Wilcox and Donner 2007). With improved homogeneity of

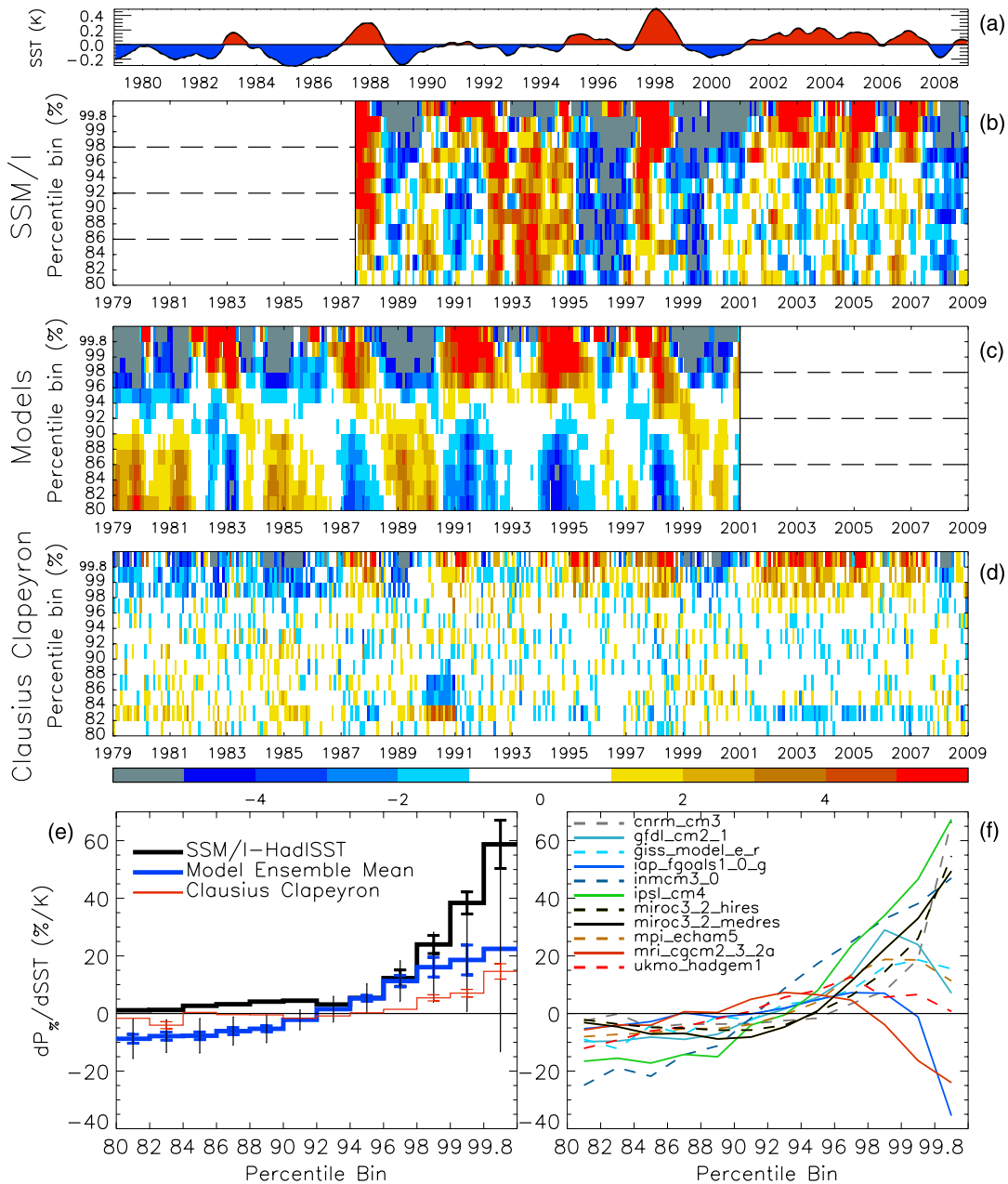


Figure 4. Interannual anomalies (smoothed by ± 2 months) of (a) observed SST (HadISST) and the frequency of daily rainfall in percentile bins of intensity ($P_{\%}$) for (b) SSM/I, (c) model ensemble mean and (d) Clausius–Clapeyron estimates based upon SSM/I data for 1990 perturbed by $7\% \text{ K}^{-1}$ observed local SST anomaly. The linear sensitivity of frequency of rainfall intensity to SST change is shown for (e) SSM/I and HadISST, the model ensemble mean and the Clausius–Clapeyron experiment and (f) individual models. In (e), standard error bars for the linear fit are plotted where correlation is significant; ± 2 standard deviations are plotted for the model data to denote the model spread.

the satellite data it will be informative to analyse trends in precipitation extremes with warming.

In summary, positive trends in the wet regions and negative trends in the dry regions of the tropics are consistent with but smaller than previous analysis (Allan and Soden 2007) and closer to model simulations. The sensitivity of the observed results to the time period and region chosen and the data set employed shows the need for further improvements in the inter-calibration and homogenization of data sets and continued inter-comparisons of different products (Adler *et al* 2001, John *et al* 2009, Smith *et al* 2009), for example from the

Tropical Rainfall Measurement Mission and CloudSat (Ellis *et al* 2009). Finally, a good physical understanding of the relationships between energy entering and stored in the climate system and the global water cycle are vital in predicting and planning for global change (Trenberth 2009, Stephens and Ellis 2008, Wild *et al* 2008, Andrews *et al* 2009).

Acknowledgments

RPA was supported by UK Natural Environment Research Council grants NE/C51785X/1 and NE/G015708/1 and the

National Centre for Earth Observation. The Met Office contribution was supported by the UK Joint DECC and DEFRA Integrated Climate Programme—GA01101. We thank two anonymous reviewers for comments leading to improvements in the analysis. GPCP data were extracted from precip.gsfc.nasa.gov and the SSM/I data from www.ssmi.com. We acknowledge the modelling groups, the Programme for Climate Model Diagnosis and Intercomparison and the World Climate Research Programme's Working Group on Coupled Modelling for their roles in making available the WCRP CMIP3 multi-model data set. Support of this data set is provided by the Office of Science, US Department of Energy.

References

- Adler R, Kidd C, Petty G, Morissey M and Goodman H 2001 *Bull. Am. Meteorol. Soc.* **82** 1377–96
- Adler R F, Gu G, Wang J J, Huffman G J, Curtis S and Bolvin D 2008 *J. Geophys. Res.* **113** D22104
- Allan R P and Soden B J 2007 *Geophys. Res. Lett.* **34** L18705
- Allan R P and Soden B J 2008 *Science* **321** 1481–4
- Allen M R and Ingram W J 2002 *Nature* **419** 224–32
- Andrews T, Forster P M and Gregory J M 2009 *J. Clim.* **22** 2557–70
- Chou C, Tu J and Tan P 2007 *Geophys. Res. Lett.* **34** L17708
- Ellis T D, L'Ecuyer T, Haynes J M and Stephens G L 2009 *Geophys. Res. Lett.* **36** L03815
- Field P R and Shutts G J 2009 *Q. J. R. Meteorol. Soc.* **135** 175–86
- Gastineau G and Soden B J 2009 *Geophys. Res. Lett.* **36** L10810
- Haerter J O and Berg P 2009 *Nat. Geosci.* **2** 372–3
- Held I M and Soden B J 2006 *J. Clim.* **19** 5686–99
- Huffman G J, Adler R F, Bolvin D T and Gu G 2009 *Geophys. Res. Lett.* **36** L17808
- John V O, Allan R P and Soden B J 2009 *Geophys. Res. Lett.* **36** L14702
- Kalnay E *et al* 1996 *Bull. Am. Meteorol. Soc.* **77** 437–71
- Lambert H F and Webb M J 2008 *Geophys. Res. Lett.* **35** L16706
- Lenderink G and van Meijgaard E 2008 *Nat. Geosci.* **1** 151–4
- Liepert B and Previdi M 2009 *J. Clim.* **22** 3156–66
- Liu S C, Fu C, Shiu C, Chen J and Wu F 2009 *Geophys. Res. Lett.* **36** L17702
- Meehl G *et al* 2007 Global climate projections *Climate Change 2007: The Physical Science Basis. Contribution of Working Group I to the Fourth Assessment Report of the Intergovernmental Panel on Climate Change* ed S Solomon, D Qin, M Manning, Z Chen, M Marquis, K B Averyt, M Tignor and H L Miller (Cambridge: Cambridge University Press) pp 747–845
- Mitchell J, Wilson C A and Cunningham W M 1987 *Q. J. R. Meteorol. Soc.* **113** 293–322
- O'Gorman P A and Schneider T 2009 *Proc. Natl Acad. Sci.* **106** 14773–7
- Pall P, Allen M R and Stone D A 2007 *Clim. Dyn.* **28** 351–63
- Petty G W 1997 *J. Geophys. Res.* **102** 1757–77
- Rayner N A, Parker D, Horton E, Folland C, Alexander L, Rowell D, Kent E and Kaplan A 2003 *J. Geophys. Res.* **108** 4407
- Smith T, Sapiano M and Arkin P 2009 *Geophys. Res. Lett.* **36** L14708
- Stephens G L and Ellis T D 2008 *J. Clim.* **21** 6141–55
- Sugiyama M, Shiogama H and Emori S 2010 *Proc. Natl Acad. Sci.* **107** 571–5
- Sun Y, Solomon S, Dai A and Portmann R W 2006 *J. Clim.* **19** 916–34
- Trenberth K E 2009 *Curr. Opin. Environ. Sust.* **1** 19–27
- Turner A G and Slingo J M 2009 *Atmos. Sci. Lett.* **10** 152–8
- Uppala S M *et al* 2005 *Q. J. R. Meteorol. Soc.* **131** 2961–3012
- Vecchi G A, Soden B J, Wittenberg A T, Held I M, Leetmaa A and Harrison M J 2006 *Nature* **441** 73–6
- Wentz F J, Ricciardulli L, Hilburn K and Mears C 2007 *Science* **317** 233–5
- Wilcox E M and Donner L J 2007 *J. Clim.* **20** 53–69
- Wild M, Grieser J and Schär C 2008 *Geophys. Res. Lett.* **35** L17706
- Yang H and Tung K K 1998 *J. Clim.* **11** 2686–97
- Zhang X, Zwiers F W, Hegerl G C, Lambert F H, Gillett N P, Solomon S, Stott P A and Nozawa T 2007 *Nature* **448** 461–5